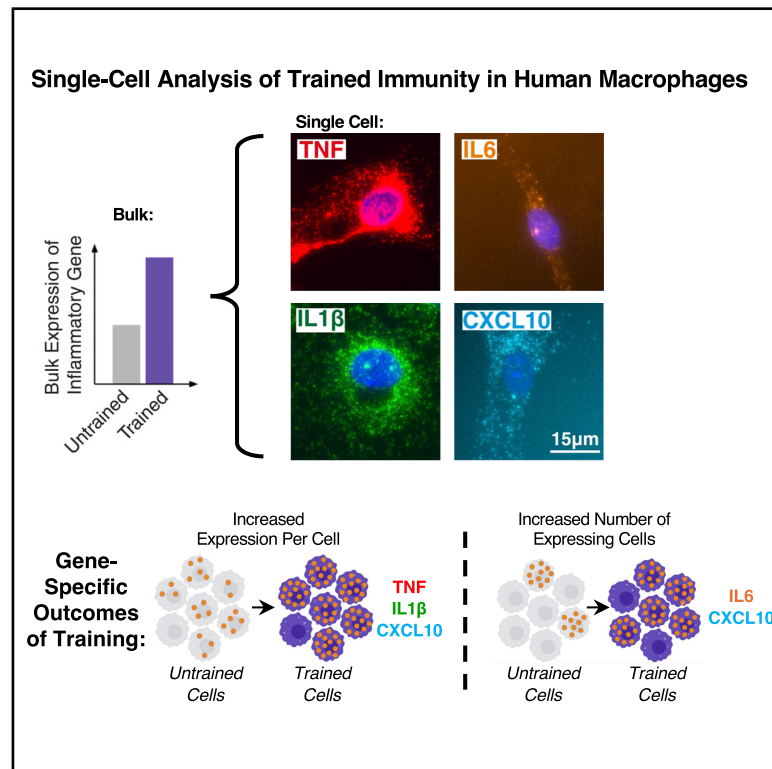


Cell Systems

Quantitative cytokine profiling of primary human macrophages reveals distinct single-cell modes of trained immunity

Graphical abstract



Authors

Aoife O'Farrell, Zijian Niu, Arjun Raj

Correspondence

arjunrajlab@gmail.com

In brief

Macrophages with prior training experiences mount stronger transcriptional responses to restimulation. Here, O'Farrell et al. reveal gene-specific single-cell transcriptional changes that generate population-wide training phenotypes in human macrophages and highlight changing time dynamics of responses that underscore the transcriptional phenotypes of trained immunity.

Highlights

- Trained immunity evaluated at single-molecule resolution in 90,000+ human macrophages
- Any single cell in the population can be trained
- Response of untrained population “catches up” to trained population at later time points
- Donor “trainability” is correlated with baseline immune activation

Article

Quantitative cytokine profiling of primary human macrophages reveals distinct single-cell modes of trained immunity

Aoife O'Farrell,¹ Zijian Niu,^{2,3,4} and Arjun Raj^{1,5,6,*}

¹Department of Bioengineering, School of Engineering and Applied Sciences, University of Pennsylvania, Philadelphia, PA, USA

²Department of Chemistry, School of Arts and Sciences, University of Pennsylvania, Philadelphia, PA, USA

³Department of Physics and Astronomy, School of Arts and Sciences, University of Pennsylvania, Philadelphia, PA, USA

⁴Computational and Systems Biology Program, Massachusetts Institute of Technology, Cambridge, MA, USA

⁵Department of Genetics, Perelman School of Medicine, University of Pennsylvania, Philadelphia, PA, USA

⁶Lead contact

*Correspondence: arjunrajlab@gmail.com

<https://doi.org/10.1016/j.cels.2026.101648>

SUMMARY

Macrophages can remember prior activation and subsequently augment their response to restimulation through trained immunity. However, it remains uncertain how trained immunity phenotypes manifest in individual cells. Here, we leverage highly quantitative single-molecule RNA imaging across 90,857 individual macrophages from 26 human donors to reveal inflammatory response dynamics in trained vs. untrained populations at single-cell resolution. Different inflammatory response genes showed distinct single-cell behavior in trained populations upon restimulation. Although training increased transcription of these response genes early after restimulation, untrained populations eventually “caught up” to the transcriptional output of trained populations, highlighting the importance of sampling timescale when interpreting transcriptional assays of training. Training did not significantly alter the relationship between the transcriptional activation of different genes within the same single cell, and any single cell appeared to be capable of training. Overall, these results revealed gene-specific single-cell transcriptional changes that generate population-wide training phenotypes in macrophages.

INTRODUCTION

Trained immunity, or training, is a form of innate immune memory whereby cells return to an inflammatory baseline following an initial stimulation but mount a stronger or faster response to restimulation. This augmented response is often demonstrated by greater production of proinflammatory cytokines and chemokines in trained cells. The majority of work establishing these differences relies on bulk genome-wide transcriptional profiling,^{1–3} qPCR for genes of interest,^{2,4,5} or bulk analysis of secreted proteins.^{3–11} Although useful in demonstrating overall phenomenology, these bulk measurements obscure potential differences in cytokine production across different individual cells, making it challenging to answer key questions about training at the single-cell level.

An increased magnitude of response to stimulation by a population of cells can stem from either graded or binary modes of single-cell variation.^{12–14} In the former, a population of cells increases the magnitude of their response through individual cells all “tuning the dial” of transcription (i.e., more transcripts of the response gene are produced per cell), and in the latter, more individual cells flip from “off” to “on” states (i.e., more single cells transcribe the response gene). Both graded and binary modes of

modulating transcription of immune response genes have been identified in immune cells, with T cells showing binary responses for interleukin (IL)-2¹⁵ and IL-4¹⁶ production and graded responses for CD25 expression¹⁷ that depend on the magnitude of the stimulation. Similarly, individual macrophages show binary dose-dependent caspase-1 activation.¹⁸ Although it is well known that trained macrophages increase transcription of immune response genes following restimulation compared with untrained cells, it is currently unknown which of these modes (graded vs. binary) is responsible for these population-wide observations and whether all trainable response genes augment transcription via the same mode.

Additionally, it currently remains unclear whether every single cell within a population is capable of being trained. Macrophages are highly heterogeneous in expression of inflammatory response genes at the single-cell level.^{19–22} This heterogeneity makes it challenging to decipher the source of variability in expression of these genes within the trained population. Variability might stem from deterministic factors (such as heterogeneous activation during the initial stimulation²³ or the presence of a cell-intrinsic property that makes some “elite” cells uniquely capable of training, as seen in other systems^{24,25}), or from probabilistic factors unrelated to the training itself.²⁶

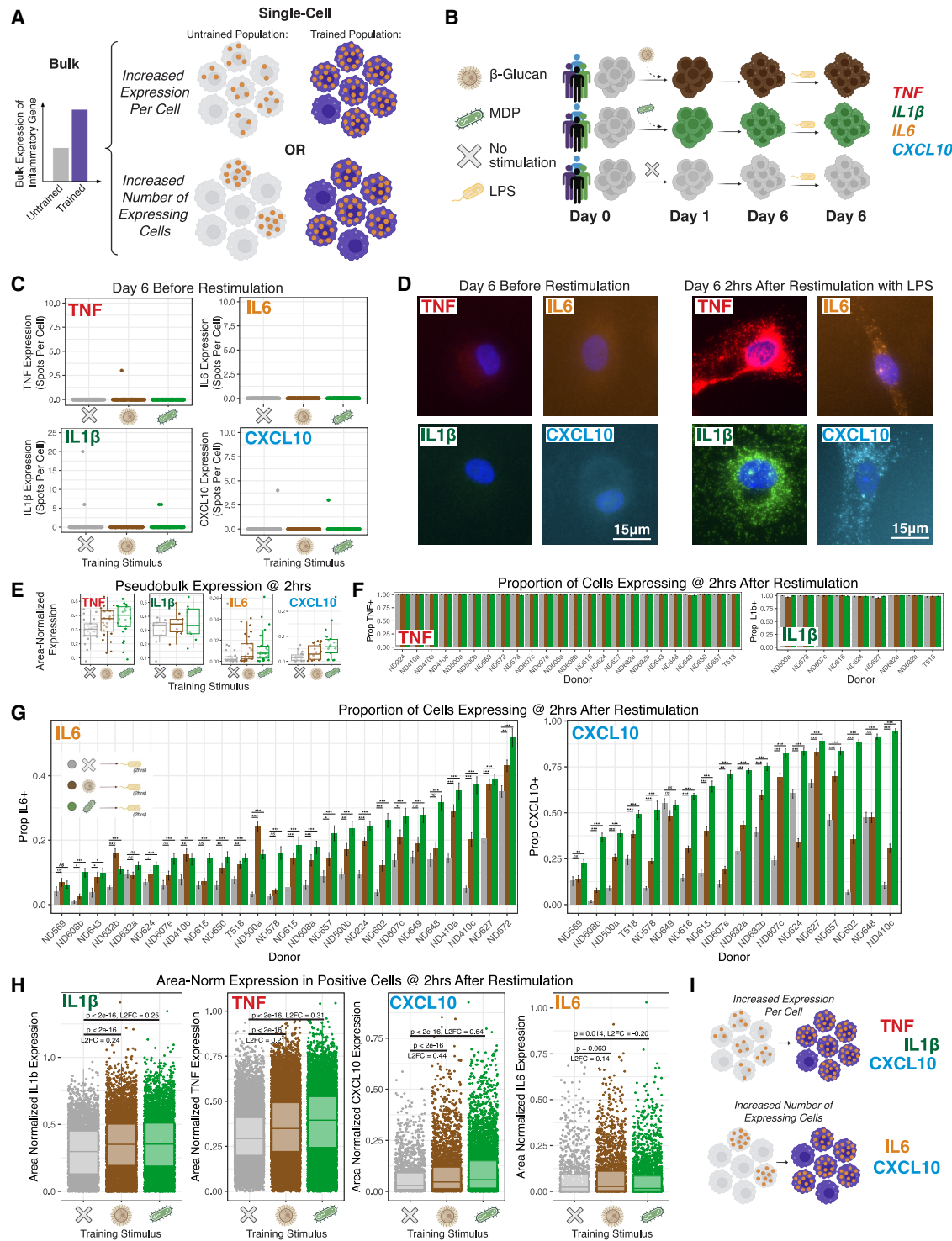


Figure 1. Single-cell cytokine expression analysis reveals distinct gene-specific modes of training

(A) Schematic of the experimental question. Bulk increase in cytokine transcription in trained populations can stem from an increase in gene transcription per single cell, or an increase in the number of cells transcribing the gene, or both.

(B) Schematic of experimental procedure. Primary human monocytes were trained with either β -glucan (5 μ g/mL) or MDP (1 μ g/mL) during the first 24 h of culture, then rested for 5 days. On day 6, cells were stimulated with 100 ng/mL lipopolysaccharide (LPS), and transcription of *TNF*, *IL1 β* , *IL6*, and *CXCL10* was assessed by RNA FISH.

(C) Transcription of *TNF*, *IL1 β* , *IL6*, and *CXCL10* in untrained (gray), β -glucan-trained (brown), or MDP-trained (green) cells on day 6 before restimulation.

(legend continued on next page)

Prior efforts to assess trained immunity at single-cell resolution have used single-cell RNA sequencing (scRNA-seq),^{27–29} which allows for measurements of the full transcriptome. However, dropout can be a significant challenge, as only a fraction of transcripts within a given cell are sequenced, and noise levels in general are high, making it difficult to make quantitative inferences for individual genes. These studies are also limited to a relatively small number of conditions owing to the resource-intensive nature of sequencing-based methods. Because trained immunity is known to differ across donors,^{10,30,31} stimuli,³² and experimental conditions,^{33,34} such results can be challenging to apply more broadly. We thus elected here to use single-molecule RNA fluorescence *in situ* hybridization (RNA FISH), which is highly accurate and quantitative and allows for the analysis of tens of thousands of cells across many conditions.

Here, we assessed the transcription of four immune response genes (*TNF*, *IL1 β* , *IL6*, and *CXCL10*) across 90,857 individual monocyte-derived macrophages, stemming from trained and untrained populations of cells across 26 human donors. We quantified differences in both the number of cells transcribing each gene and the amount of transcripts produced per cell to reveal that different genes have different modes of increasing transcription in trained macrophages following restimulation. We identified cross-gene relationships within single cells that are maintained with training, suggesting that any cell is capable of being trained by the initial stimulation. We compared the transcriptional response to restimulation at early (2 h) and later (6 h) time points, which revealed that untrained populations “catch up” to the transcriptional output of trained populations at later time points, suggesting that these trainable genes may respond more quickly but not necessarily more strongly to restimulation. Overall, our quantitative analysis of the trained response in primary human macrophages revealed that training has gene-specific effects upon the population distribution of the transcriptional response to restimulation and that this response is also highly dynamic, suggesting that timing (as opposed to absolute output at any given time) is a critical aspect of the trained response.

RESULTS

Single-cell cytokine expression analysis reveals distinct gene-specific modes of training

Trained macrophages increase transcription of many proinflammatory response genes following restimulation, compared with

their untrained counterparts. This increase in expression could stem from an increased transcriptional output per individual cell (graded), from an increase in the number of single cells that have turned on expression of that gene (binary), or a combination of both (Figure 1A). We wanted to determine which of these modes applied to inflammatory response genes in trained macrophages.

We generated trained macrophages using a highly controlled, well-established *in vitro* protocol.^{1,4,6,27,33} Briefly, we collected monocytes from the apheresis product of healthy human donors, stimulated with a training stimulus on the first day of culture, then washed out this training stimulus after 24 h. We then allowed the cells to rest for 5 additional days before assessing their gene expression on day 6 (Figure 1B). We generated trained monocyte-derived macrophages using two different training ligands—the fungal-protein β -glucan and the bacterial mimetic muramyl dipeptide (MDP)—to determine whether single-cell characteristics of training were shared across trained states. For evaluation of differences in the trained state induced by different training stimuli, please see our companion manuscript.³⁵

We evaluated the expression of four inflammatory response genes: *TNF*, *IL1 β* , *CXCL10*, and *IL6*. These genes were selected because prior literature has shown their expression to be trainable,^{2,6,36} induced in macrophages upon stimulation with lipopolysaccharide (LPS),³⁷ and highly heterogeneous across individual macrophages.^{27,38} Single-molecule RNA FISH allowed for highly accurate quantification of transcription of these four genes in absolute molecular units with single-cell resolution in 90,857 cells spread across 3 training conditions (untrained, β -glucan-trained, and MDP-trained), 8 time points, and 26 human donors.

We first confirmed that trained cells were not expressing any of these response genes on day 6 while at a resting state. Indeed, we found virtually no expression of *TNF*, *IL1 β* , *CXCL10*, or *IL6* before restimulation (Figure 1C). Transcription of all four genes was rapidly induced in both trained and untrained cells following restimulation with LPS 6 days after training (Figure 1D). When we analyzed the mean expression of *TNF*, *IL1 β* , *CXCL10*, and *IL6* 2 h after restimulation, we found that expression of all four genes was greater in trained populations than in untrained populations (Figure 1E). These properties—a return to inflammatory baseline followed by a stronger response to secondary stimulation—are hallmarks of training memory, as opposed to other forms of innate immune memory such as priming or tolerance.³⁹

(D) Representative RNA FISH images of *TNF*, *IL1 β* , *IL6*, and *CXCL10* expression before (left) and 2 h after (right) restimulation with LPS. Donors shown before restimulation are ND410a and ND652, and at 2 h is ND500a. Images are representative of approx. 400 cells per condition.

(E) Averaged RNA FISH data across cells showing mean area-normalized expression of *TNF*, *IL1 β* , *IL6*, and *CXCL10* in untrained (gray), β -glucan-trained (brown), and MDP-trained (green) populations 2 h after restimulation with LPS. $n = 24$ donors for *TNF*, 9 donors for *IL1 β* , 26 donors for *IL6*, and 18 donors for *CXCL10*.

(F) Proportion of cells expressing *TNF* (left) and *IL1 β* (right) in untrained (gray), β -glucan-trained (brown), and MDP-trained (green) populations 2 h after restimulation with LPS. Error bars show the standard error of percentage.

(G) Proportion of cells expressing *IL6* (left) and *CXCL10* (right) in untrained (gray), β -glucan-trained (brown), and MDP-trained (green) populations 2 h after restimulation with LPS. Error bars show the standard error of percentage. Statistics: *** $p < 0.001$, ** $p < 0.01$, * $p < 0.05$, NS $p > 0.05$.

(H) Area-normalized transcripts per cell of *TNF*, *IL1 β* , *IL6*, and *CXCL10* for expressing cells (counts above zero) in untrained (gray), β -glucan-trained (brown), and MDP-trained (green) populations 2 h after restimulation with LPS. Data concatenated across donors; data split by individual donor in Figure S2. p value and \log_2 fold change calculated between each trained condition vs. untrained cells.

(I) Summary schematic. Training of *TNF*, *IL1 β* , and *CXCL10* appears to stem from increased transcriptional output per cell, while training of *IL6* and *CXCL10* appears to stem from increased number of transcribing single cells.

Number of single cells analyzed per condition can be found in Table S3.

We then assessed this data at single-cell resolution to identify how training boosted transcription at the single-cell level. 2 h after restimulation with LPS, almost every individual cell in both trained and untrained populations had turned on expression of *TNF* and *IL1 β* (Figure 1F). Even just 30 min after stimulation with LPS, 100% of cells expressed *TNF* and 78% expressed *IL1 β* (Figure S1A). However, only a subset of single cells had begun expressing *IL6* (9% of untrained cells) and *CXCL10* (27% of untrained cells) at 2 h post restimulation. We dubbed these cells “first responders,” as they were likely the first in the population to begin expressing these genes. The proportion of first responder cells in the population increased following training with β -glucan or MDP as compared with untrained cells (Figure 1G). We found a statistically significant increase in the proportion of cells expressing *IL6* in 19 of 26 assessed donors for β -glucan training and in 24 of 26 donors for MDP training. For *CXCL10*, 14 of 18 donors for β -glucan training and 17 of 18 donors for MDP training showed a statistically significant increase in the proportion of cells expressing that gene. We also found an association between a cell's morphology and its propensity to be a first responder—cells with a smaller area and with greater eccentricity were more likely to express *IL6* at 2 h post restimulation across both trained and untrained populations (Figure S1B).

We next wanted to measure the changes in transcriptional output of genes specifically in the subset of expressing cells (excluding non-expressing cells). As such, we removed any cell not expressing a gene (for which the transcript count was zero) and quantified expression per cell. We noted that raw transcript count and total cell area were correlated (Figure S1C). To compensate for this effect,⁴⁰ we quantified transcription per cell by normalizing the number of transcripts per cell by that cell's area.

We found that the mean expression per cell in the expressing subpopulation increased with training for *TNF*, *IL1 β* , and *CXCL10* but not *IL6* (Figure 1H). Although subject to greater noise due to smaller cell number and donor heterogeneity, we also observed this same trend on a donor-by-donor basis (Figure S2). Mean *TNF* expression was statistically significantly higher in trained cells for 63% of donors (15 of 24) for β -glucan training and 80% of donors (19 of 24) for MDP training. For *IL1 β* , significantly higher in trained cells for 67% of donors (6 of 9) for β -glucan training and 78% (7 of 9) for MDP. For *CXCL10*, significantly higher in trained cells for 50% of donors (9 of 18) for β -glucan training and 56% (10 of 18) for MDP. We only observed a statistically significant increase in expression of *IL6* in 35% of donors (9 of 26) for either β -glucan or MDP training.

Together, these results illustrate distinct single-cell modes of training for different immune response genes 2 h after restimulation. Increased *TNF* and *IL1 β* expression stems from a graded increase in transcriptional output from individual cells in the population. Training of *IL6*, however, appears to primarily stem from a binary increase in the number of responding single cells. Increased expression of *CXCL10* in trained cells stems from both increased output per cell and increased number of cells in the population expressing the gene (a both graded and binary change).

Any single cell can be trained

Although training induced an overall upward shift in the distribution of expression of several genes, not every cell showed an increase in expression above untrained population averages. This heterogeneity raised the possibility that only some “elite” individual cells within the population are trained while others remain untrained, as has been suggested previously.²⁷ To that end, we wanted to determine whether such an elite subpopulation of trainable cells existed within populations exposed to a training stimulus. Alternatively, it could be that every cell is capable of undergoing training but that some cells simply do not express cytokine at that one moment in time due to other probabilistic factors^{26,41} (Figure 2A).

To distinguish between these possibilities, we reasoned that if a privileged subpopulation of trainable cells existed, those cells would have higher levels of expression of multiple markers of training (e.g., express both *IL6* and *CXCL10* at 2 h) compared with the remaining untrained cells in the population. If, on the other hand, the entire population was able to train and the heterogeneity from cell to cell reflected other factors unrelated to training, then we would expect an overall lack of correlation between the expression of multiple cytokines across the population, because each cell's expression would merely reflect some instantaneous probabilistic factor rather than a specific entrained state. We therefore returned to our first responder cells producing *IL6* or *CXCL10* at 2 h after restimulation with LPS (Figures 2B and 2C). At the population level, elite cells would manifest as a higher number of doubly positive cells for the two genes than expected by random chance (Figure 2D). Quantitatively, this association can be captured with the log₂ odds ratio of expression for the two genes, which would be greater in trained populations as compared with untrained populations.

However, we instead observed that the log₂ odds ratio for expression of *IL6* and *CXCL10* at 2 h was nearly identical between trained and untrained populations (Figure 2E). This value was above zero: cells that were first responders for one gene were slightly more likely to also be first responders for the other, although the association was not strongly predictive. First responders for *IL6* were ~2 times more likely to also express *CXCL10* than cells not expressing *IL6*, and first responders for *CXCL10* were ~3 times more likely to also express *IL6* than cells not expressing *CXCL10*. However, despite the increased number of cells expressing either gene in trained populations, the association between the two genes within the same cell did not change with training. As such, the association between early expression of *IL6* and *CXCL10* within the same cell following stimulation with LPS may represent a fundamental aspect of macrophage biology that is unaffected by training.

The extremely similar odds ratios for *IL6* and *CXCL10* expression in trained and untrained cells indicated there was not an elite subpopulation of trainable cells, showing that any single cell in the population was capable of building memories of prior stimulation. We also found that the magnitude of expression of *TNF* vs. *IL6*, *TNF* vs. *CXCL10*, and *IL1 β* vs. *CXCL10* had low correlation in single cells at these early time points (Figure S3A), providing further evidence against an elite subset of trainable cells driving memory phenotypes in the population.

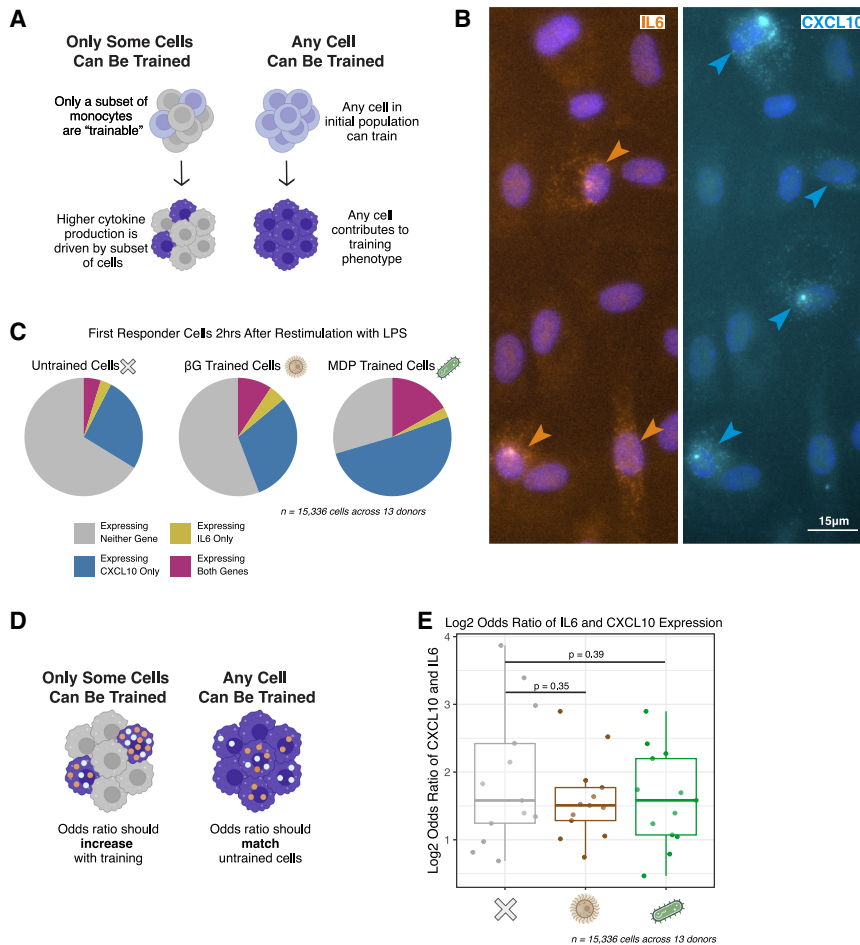


Figure 2. Any single cell can be trained

(A) Schematic of the experimental question. If only a subset of monocytes is trainable, a memory phenotype should only be present in a subset of macrophages 6 days later.

(B) Representative RNA FISH image of first responder cells expressing *IL6* or *CXCL10* 2 h after restimulation with LPS, with responding cells indicated by arrows. Donor shown is ND648, and cells are from the β-glucan-trained population. Images are representative of approx. 350 cells per condition.

(C) Proportion of untrained, β-glucan-trained, and MDP-trained cells expressing *CXCL10*, *IL6*, neither, or both 2 h after restimulation with LPS. Data concatenated across 13 donors.

(D) Schematic of experimental question. If only some cells can train, there should be an over-representation of double-positive cells, with a higher log₂ odds ratio of expression of *IL6* and *CXCL10* in single cells from trained populations. If any cell trains, the log₂ odds ratio of expression of these genes should not increase in trained populations.

(E) Log₂ odds ratio of *CXCL10* and *IL6* expression in untrained (gray), β-glucan-trained (brown), and MDP-trained (green) cells 2 h after stimulation with LPS. n = 13 donors.

Number of single cells analyzed per condition can be found in Table S3.

In two donors, we performed a more fine-grained time course analysis, sampling *TNF* and *IL6* transcription in trained and untrained cells every hour for 6 h after restimulation with LPS (Figure 3F).

Transcriptional output from trained cells decreases at later points in the inflammatory response

We next wanted to determine whether the transcriptional trends observed 2 h after restimulation with LPS (namely, increased expression of proinflammatory response genes driven by both graded and binary modes and an unchanged odds ratio of *IL6* and *CXCL10* expression across single cells) were also present at later time points in the inflammatory response. To do so, we quantified transcription of *TNF*, *IL1β*, *CXCL10*, and *IL6* in trained and untrained populations 6 h after restimulation with LPS and compared these data to our 2 h time point (Figure 3A).

We first noticed that the proportion of cells expressing *IL6* and *CXCL10* in untrained populations began to “catch up” to what we observed in our trained populations (Figures 3B and 3C). Expression of *TNF* and *IL1β* remained high across trained and untrained populations (95%–100% of cells), while around 75% of cells expressed *CXCL10* and around 50% expressed *IL6* 6 h after restimulation.

We next quantified the transcriptional output per cell for the expressing cells (with counts above zero for the gene of interest) 6 h after restimulation. We found that transcriptional output per expressing cell was notably lower in trained populations than in untrained populations across all four genes (with the trend particularly noticeable for *TNF* and *IL6* expression) (Figures 3D, 3E, and S4A).

Intriguingly, when we computed the area under the expression curve for trained and untrained populations as a proxy for the total expression of these genes across the response to restimulation, we found these values to be similar between trained and untrained cells. This may suggest that training generates a transcriptional response for *TNF* and *IL6* that is faster but not necessarily stronger in aggregate following restimulation with LPS.

At these later points in the transcriptional response to restimulation, trained cells showed decreased expression per cell compared with what was seen in the untrained population. We wondered if this decrease in expression may be due to paracrine signaling from nearby cells activating negative feedback loops to avoid immune overreaction, as occurs through quorum sensing.^{19,22} We found that increased local cell density (taken from natural variation from where cells resided on the dish) was negatively correlated with *IL6* and *TNF* expression (but not *CXCL10* expression) only in trained populations at 6 h post restimulation (Figure S4B). These correlations were not present in either trained or untrained populations 2 h after restimulation. This finding supports the hypothesis that decreased expression of these response genes in trained cells at later time points in the inflammatory response may be due to faster initial production and thus faster activation of negative feedback mechanisms from

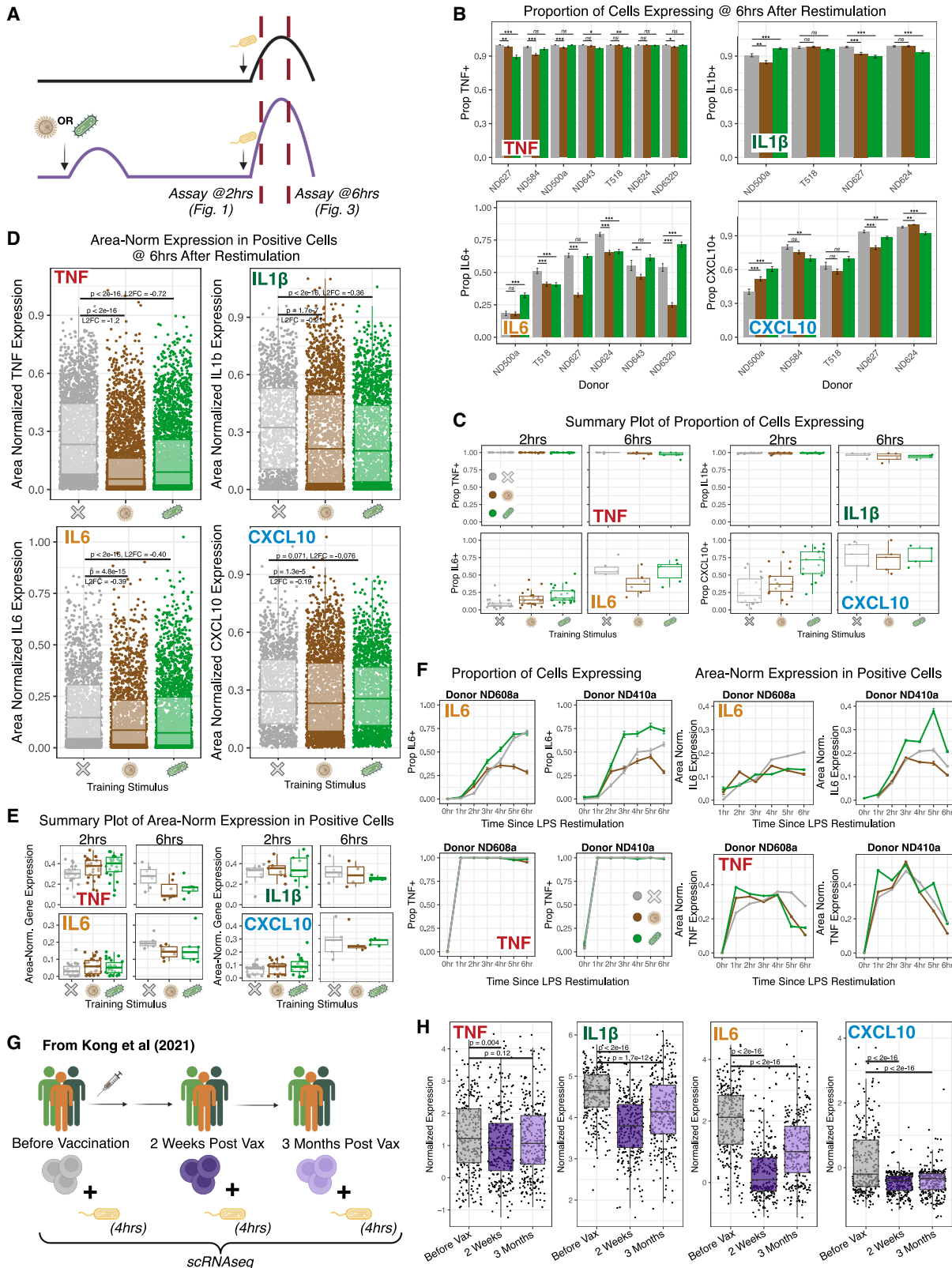


Figure 3. Transcriptional output from trained cells decreases at later points in the inflammatory response

(A) Schematic of experimental procedure. *TNF*, *IL1β*, *IL6*, and *CXCL10* transcription in trained and untrained cells was assessed by RNA FISH 2 and 6 h after restimulation with 100 ng/mL LPS.

neighboring cells as the population moves to restore inflammatory baseline following stimulation.

At 6 h post restimulation with LPS, we found that the odds ratio of expression of *IL6* and *CXCL10* in single cells was similar between trained and untrained cells, as it also was at 2 h post restimulation (Figure S3C). The odds ratio between the expression of these two genes was slightly lower at 6 h than it was at 2 h post restimulation. Cells expressing *IL6* were ~ 1.2 times more likely to also express *CXCL10* than cells not expressing *IL6*, and cells expressing *CXCL10* were ~ 2 times more likely to also express *IL6* than cells not expressing *CXCL10*. We also found that cells expressing *IL6*, on average, expressed a greater magnitude of *TNF* than cells not expressing *IL6*, across trained and untrained cells at 6 h post restimulation (Figure S4C). This relationship between *TNF* and *IL6* expression was true in untrained, but not trained, populations at 2 h. Together, these results demonstrated that an elite subpopulation driving trained phenotypes did not emerge in trained populations at later time points in the response to restimulation.

Our experiments quantified training within a highly controlled, *in vitro* setting. We wondered whether similar trends might be present in single cells following training *in vivo*, where additional variables may influence training behavior. We analyzed a published scRNA-seq dataset of 1,710 human monocytes collected immediately before, 2 weeks, and 3 months following training with the Bacillus Calmette-Guérin (BCG) vaccine in three human donors.²⁸ We then filtered this dataset to the 855 monocytes assessed 4 h after an *ex vivo* restimulation with LPS (Figure 3G). Trained monocytes from this dataset showed lower production of *IL1 β* , *TNF*, *IL6*, and *CXCL10* compared with samples taken before vaccination (Figure 3H). We also found similar trends of lower expression in trained cells for additional genes associated with training within this dataset, including other chemokines and cytokines, metabolism-associated genes, and antigen presentation machinery (Figure S4D). These findings corroborate our *in vitro* training data, demonstrating that at later time points after a restimulation, trained cells show reduced transcription of key proinflammatory response genes.

Training capacity varies across individuals and is negatively associated with baseline state

Thus far, we have primarily discussed trends in single-cell heterogeneity in the transcription of inflammatory response genes

that held across most donors in aggregate. However, we noticed substantial differences in the degree of training observed across individual donors in our analysis. We defined a summary metric called the “training capacity,” which quantifies changes to cells due to training, to measure donor variability in training across our datasets (Figures 4A and 4B). The training capacity is defined as the \log_2 fold change of mean area-normalized expression between trained and untrained cells for *TNF* and *IL1 β* 2 h after LPS restimulation and the \log_2 fold change of proportion of expressing cells between trained and untrained cells for *IL6* and *CXCL10* 2 h after LPS restimulation, to reflect the distinct modes of training for these genes. Donors with a higher training capacity had a larger boost in cytokine expression upon restimulation when comparing trained to untrained cells, while those with a lower training capacity showed similar expression levels between trained and untrained cells.

Although β -glucan and MDP generated different memory states, we found the training capacity for either stimulus within the same donor to be strongly correlated (donors with strong phenotypic changes from training with one stimulus also showed strong phenotypic changes from training with the other). Within the same donor, training at different loci was also generally correlated (donors with large changes in *IL6* at the population level due to training also showed large changes in *CXCL10*) (Figure 4C).

We observed a strong negative association between a donor's untrained (baseline) response to restimulation and their training capacity for *IL6* and *CXCL10*, but not *TNF* (*IL1 β* showed a stronger association in β -glucan-trained cells than MDP-trained cells) (Figures 4D and S5B). Macrophages from donors who had a low baseline inflammatory response saw a greater boost in expression from training: the two donors with the lowest *IL6* expression in the untrained condition had training capacities of 3.57 and 2.65 for training with MDP, while the two donors with the highest untrained *IL6* expression had training capacities of 0.56 and 0.92 for training with MDP. This trend could suggest that donors with low capacity may have preexisting memory of some prior inflammatory experience and are already in a trained state at the time of sample collection. As such, further training would do little to further boost cytokine production (i.e., they have reached a ceiling of maximal expression). Training capacity did not seem to depend on donor age or sex, or the time of year of sample

(B) Proportion of cells expressing *TNF*, *IL1 β* , *IL6*, and *CXCL10* in untrained (gray), β -glucan-trained (brown), and MDP-trained (green) populations 6 h after restimulation with LPS. Error bars show the standard error of percentage. Statistics: *** $p < 0.001$, ** $p < 0.01$, * $p < 0.05$, NS $p > 0.05$.

(C) Summary plot of data shown in Figures 1F and 1G and (B), directly comparing the proportion of cells expressing *TNF*, *IL1 β* , *IL6*, and *CXCL10* in trained and untrained populations at 2 h vs. 6 h after restimulation with LPS. Each data point shows the proportion of the population expressing each gene as observed in one donor.

(D) Area-normalized transcripts per cell of *TNF*, *IL1 β* , *IL6*, and *CXCL10* for expressing cells (counts above zero) in untrained (gray), β -glucan-trained (brown), and MDP-trained (green) populations 6 h after restimulation with LPS. Data concatenated across donors; data split by individual donor in Figure S4A.

(E) Summary plot of data shown in Figure 1H and (D), directly comparing the mean area-normalized transcripts per expressing cell of *TNF*, *IL1 β* , *IL6*, and *CXCL10* at 2 h vs. 6 h after restimulation with LPS. Each data point shows the mean area-normalized transcripts per expressing cell as observed in one donor.

(F) Time course analysis of *TNF* and *IL6* expression (proportion of cells expressing [left] and area-normalized transcripts per expressing cell [right]) in untrained (gray), β -glucan-trained (brown), and MDP-trained (green) populations for two donors. Error bars show the standard error of percentage (left) and standard error of the mean (right).

(G) Schematic of experimental procedure from published single-cell RNA sequencing (scRNA-seq) dataset by Kong et al.²⁸ Human monocytes were collected from the blood of three human donors immediately before, 2 weeks after, and 3 months after BCG vaccination. Cells were then stimulated *ex vivo* for 4 h with LPS and then underwent scRNA-seq.

(H) Expression of *TNF*, *IL1 β* , *IL6*, and *CXCL10* in monocytes before (untrained control, gray), 2 weeks after (purple), and 3 months after (lilac) BCG vaccination, following a 4-h stimulation with LPS, by scRNA-seq.

Number of single cells analyzed per condition can be found in Table S3.

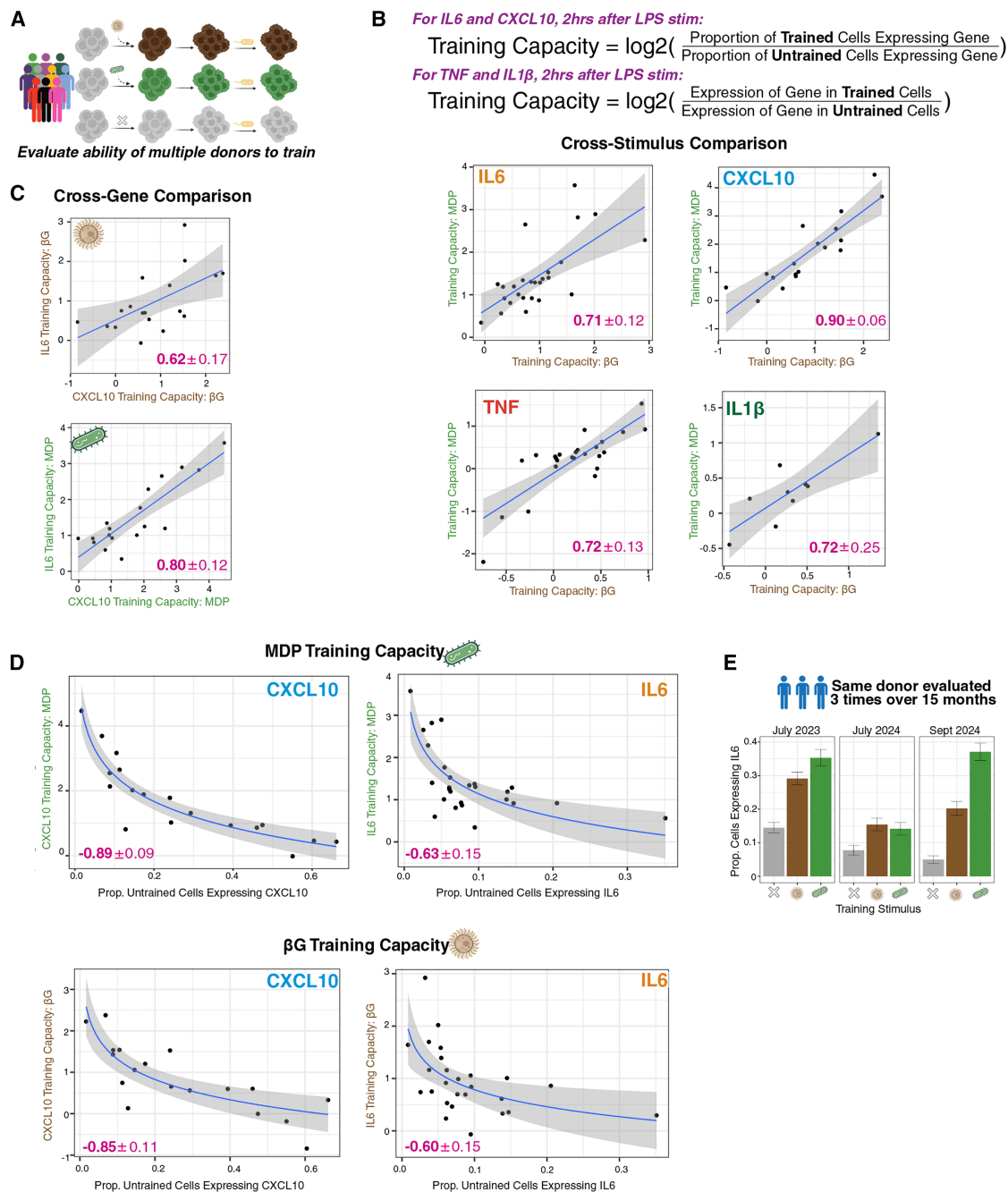


Figure 4. Training capacity varies across individuals and is negatively associated with baseline state

(A) Schematic of experimental procedure. Cells from 26 human donors were trained with β -glucan or MDP for the first 24 h of culture. Gene expression was assessed 2 h after stimulation with 100 ng/mL LPS.

(B) Top: equations used to calculate training capacity. Bottom: training capacity for β -glucan vs. MDP in the same donor for *IL6*, *CXCL10*, *IL1β*, and *TNF*. Pink text shows Spearman's correlation coefficient plus or minus the standard error (by bootstrap) between variables.

(C) Training capacity for *IL6* vs. *CXCL10* in the same donor for β -glucan and MDP. Pink text shows Spearman's correlation coefficient plus or minus the standard error (by bootstrap) between variables.

(D) Association between training capacity for *CXCL10* (left) and *IL6* (right) and proportion of cells expressing cytokine in the untrained condition for each donor. Pink text shows Spearman's correlation coefficient plus or minus the standard error (by bootstrap) between variables.

(E) Proportion of cells expressing *IL6* in untrained (gray), β -glucan-trained (brown), or MDP-trained (green) populations, 2 h after stimulation with LPS, for the same donor evaluated 3 times (ND410a, ND410b, ND410c). Error bars show the standard error of percentage.

Number of single cells analyzed per condition can be found in [Table S3](#).

collection (Figure S5A); however, our sample size is likely insufficient to fully support a lack of correlation between these variables and the training capacity of a donor.

It has been suggested that differences in training ability across individuals may be due to genetic differences³¹ or non-genetic differences.³⁰ To measure the influence of these variables, we profiled cells from the same individual 3 times over the course of 15 months. We found that this donor's transcriptional response to restimulation varied widely across the three sample dates (*IL6* training capacity ranging from 0.87 to 2.89 for training with MDP) and that the baseline (untrained) response also varied widely over time (Figure 4E). We saw similar variability for four donors profiled twice over the course of several months (Figure S5C). These findings suggest that transient non-genetic variation may play a larger role than genetic differences in the degree of phenotypic change due to training in an individual donor.

DISCUSSION

Here, we describe changes to transcriptional regulation that occur due to training for four immune response genes in primary human macrophages. Memory of prior immune activation alters both the number of cells producing cytokines and chemokines early in the inflammatory response, as well as the transcriptional output per cell, in a gene-specific manner. However, at later time points following restimulation, transcriptional output per cell in trained populations fell below what is seen in untrained cells. Despite these changes in mean output, both trained and untrained populations displayed sizable cell-cell heterogeneity in transcription of these genes.

We demonstrate distinct modes of tuning immune response gene transcription in trained cells within a highly controlled, *in vitro* context. This experimental setup ensured each single cell experienced the same magnitude of both the training stimulus and the LPS restimulation, which cannot be ensured in a complex *in vivo* tissue environment. Although we were able to corroborate some of our single-cell findings in a human *in vivo* trained immunity dataset (namely, a lower transcriptional output per trained cell of many immune response genes at later time points post restimulation), it remains unknown whether all the single-cell features of training identified here apply in an *in vivo* environment. We also note that our graded vs. binary distinctions were observed at a relatively high dose of LPS restimulation; it is possible that different patterns may emerge at different doses of LPS or following restimulation with different stimuli.

Overall, our findings highlight the importance of sample collection time when interpreting transcriptional changes to macrophages due to memory of prior exposures. As demonstrated here, the same memory-inducing stimulus may be viewed as inducing training (greater expression than untrained cells) or tolerance (less expression than untrained cells), depending on the time at which transcription of these genes was assessed. We suggest that the timescales of these responses should be considered carefully when making qualitative assessments of trained vs. tolerant memory responses.

Although the traditional RNA FISH method employed here provides highly quantitative information about the four genes

profiled, we were limited to only a small number of genes. It remains unknown whether other trainable genes, including other cytokines and chemokines, manifest bulk increases in transcription as a greater output per cell or as a greater number of producing cells.

Transcriptional output (measured either as the number of transcribing cells or the number of transcripts per cell) significantly increased in trained populations at 2 h post restimulation, but the magnitude of change from untrained populations shown here was relatively small (\log_2 FC of 0.31 for *TNF*, 0.25 for *IL1 β* , and 0.64 for *CXCL10* transcriptional increase with training with MDP). Published literature evaluating secreted protein for these genes generally reveals a larger magnitude of change between trained and untrained populations (\log_2 FC typically ranging between 1 and 4 for *IL6* and *TNF* secretion comparing trained to untrained cells).^{1,3–6,11} These differences may be due to additional post-transcriptional regulation of the production of these proteins. Alterations to metabolic pathways are also known to play a significant role in trained immunity, which may affect how cytokines and chemokines are translated and secreted,^{42–45} thus magnifying relatively smaller transcriptional changes into larger differences in protein output.

At 6 h post restimulation, we noted that trained cells were transcribing proinflammatory response genes at lower levels than untrained cells. There are a multitude of potential explanations for this result. It could be that faster production of these cytokines, and thus faster secretion into the local environment, activates negative feedback loops more quickly in trained populations (in support of this hypothesis, more dense local environments of trained cells saw less *IL6* and *TNF* expression). However, it could also be that trained cells are faster to turn on anti-inflammatory pathways in addition to proinflammatory ones. It has been previously observed that trained cells produce more of the anti-inflammatory cytokine *IL10* than untrained cells.^{4,7}

Based on our analysis of first responder cells in Figure 2, we showed that any individual macrophage is seemingly capable of building memory of prior stimulation. However, it is still possible that some individual cells have a stronger magnitude of change in their phenotypic response to restimulation (their “decoding” of memory) than others; i.e., that there is some variability in training capacity on a per cell basis. With our current experimental setup (particularly, the use of primary human cells), we cannot determine the degree of transcriptional change of an individual cell due to training, as heterogeneity across single cells in both trained and untrained populations leaves us unable to determine what that cell's transcriptional state “would have been” had it not been trained. Retrospective analysis via the tracking of recently-divided sister cells (which more closely resemble each other transcriptionally than the bulk population) by training one sister cell and comparing its response to restimulation against its untrained sister^{24,25,46} may allow for such conclusions to be drawn in the future.

RESOURCE AVAILABILITY

Lead contact

Requests should be directed to and will be fulfilled by the lead contact, Arjun Raj (arjunrajlab@gmail.com).

Materials availability

This study did not generate any new reagents.

Data and code availability

- All code used to analyze data and generate figures can be found on Dropbox at <https://www.dropbox.com/scl/fo/q5jt87fhviyv4ygtvgvqqt/AObPxxHcmDGD6RixA8Z7NQE?rlkey=sfqf8w9wewcq1zlte6xbueixo&st=d0m469u5&dl=0> and on Data Dryad at <https://doi.org/10.5061/dryad.stjq2cjc> and is publicly available as of the date of this publication.
- Any additional information required to reanalyze the data reported in this paper is available from the [lead contact](#) upon request.

ACKNOWLEDGMENTS

The authors would like to thank members of the Raj Lab for scientific discussion and detailed commentary on the manuscript, in particular Serena El Feghali, Laura Van Eyndhoven, Pavithran Ravindran, Grant Kinsler, Gianna Busch, and Catherine Triandafillou; Dr. Sunny Shin for expert guidance on macrophage biology; and summer research students Juan McCook and Nava Graham for scientific discussion and collaborative efforts. Figure cartoons were created using [Biorender.com](https://biorender.com).

The authors thank Emily Cento, Zhilin Chen, Max A. Eldabbas, and Emileigh Maddox of the Human Immunology Core and the Division of Transfusion Medicine and Therapeutic Pathology at the Perelman School of Medicine at the University of Pennsylvania for providing de-identified monocytes that were purified from healthy donor apheresis using StemCell RosetteSep kits. The HIC is supported in part by NIH P30 AI045008 and P30 CA016520; HIC RRID: SCR_022380.

A.R. acknowledges support from a center grant from the Mark Foundation for Cancer Research and an NIH Director's Transformative Research Award R01 GM137425. A.O. acknowledges support from NSF GRFP DGE-2236662. This project was made possible through the support of grant 63532 from the John Templeton Foundation. Z.N. acknowledges support from the Roy and Diana Vagelos Scholars Program in the Molecular Life Sciences, the Roy and Diana Vagelos Science Challenge Award, the Barry M. Goldwater Scholarship, the Fannie and John Hertz Foundation Fellowship, the Paul & Daisy Soros Fellowship for New Americans, and the Department of Energy Computational Science Graduate Fellowship.

AUTHOR CONTRIBUTIONS

A.O. and A.R. conceived the project and designed all experiments. Z.N. and A.R. developed image analysis software for all image analyses used in this manuscript, including automated RNA FISH spot detection. A.O. and A.R. prepared all illustrations and wrote the manuscript, with input from all authors.

DECLARATION OF INTERESTS

A.R. receives royalties related to Stellaris RNA FISH probes. A.R. serves on the scientific advisory board of Spatial Genomics and is an employee of Somite Therapeutics while on sabbatical leave.

DECLARATION OF GENERATIVE AI AND AI-ASSISTED TECHNOLOGIES IN THE WRITING PROCESS

During the preparation of this work, the authors used Claude to generate and comment code for analyses. After using this tool or service, the authors reviewed and edited the content and take full responsibility for the content of the publication.

STAR★METHODS

Detailed methods are provided in the online version of this paper and include the following:

- [KEY RESOURCES TABLE](#)

● EXPERIMENTAL MODEL AND STUDY PARTICIPANT DETAILS

● METHOD DETAILS

- Induction of trained immunity
- Single-molecule RNA fluorescence in-situ hybridization (RNA FISH) image acquisition
- Single-molecule RNA fluorescence in-situ hybridization (RNA FISH) image analysis
- Single cell RNA sequencing data analysis

● QUANTIFICATION AND STATISTICAL ANALYSIS

SUPPLEMENTAL INFORMATION

Supplemental information can be found online at <https://doi.org/10.1016/j.cels.2026.101648>.

Received: January 31, 2025

Revised: October 20, 2025

Accepted: May 27, 2026

REFERENCES

1. Novakovic, B., Habibi, E., Wang, S.-Y., Arts, R.J.W., Davar, R., Megchelenbrink, W., Kim, B., Kuznetsova, T., Kox, M., Zwaag, J., et al. (2016). β -Glucan Reverses the Epigenetic State of LPS-Induced Immunological Tolerance. *Cell* 167, 1354–1368.e14. <https://doi.org/10.1016/j.cell.2016.09.034>.
2. Adamson, M.S., Nestic, S., Buness, A., Bayrak, K., Schmitz, S., Soler, S., Zillinger, T., Marx, S., Lambing, S., Andryka-Cegielski, K., et al. (2022). RIG-I activation primes and trains innate antiviral immune memory. Preprint at bioRxiv. <https://doi.org/10.1101/2022.10.27.514004>.
3. Cheng, Q.J., Farrell, K., Fenn, J., Ma, Z., Mankanani, S.K., and Siemsen, J. (2024). Dectin-1 ligands produce distinct training phenotypes in human monocytes through differential activation of signaling networks. *Sci. Rep.* 14, 1454. <https://doi.org/10.1038/s41598-024-51620-8>.
4. Carlile, S.R., Cahill, S.C., O'Brien, E.C., Neto, N.G.B., Monaghan, M.G., and McLoughlin, R.M. (2024). *Staphylococcus aureus* induced trained immunity in macrophages confers heterologous protection against gram-negative bacterial infection. *iScience* 27, 111284.
5. Bekkering, S., Quintin, J., Joosten, L.A.B., van der Meer, J.W.M., Netea, M.G., and Riksen, N.P. (2014). Oxidized low-density lipoprotein induces long-term proinflammatory cytokine production and foam cell formation via epigenetic reprogramming of monocytes. *Arterioscler. Thromb. Vasc. Biol.* 34, 1731–1738. <https://doi.org/10.1161/ATVBAHA.114.303887>.
6. Ifrim, D.C., Quintin, J., Joosten, L.A.B., Jacobs, C., Jansen, T., Jacobs, L., Gow, N.A.R., Williams, D.L., van der Meer, J.W.M., and Netea, M.G. (2014). Trained immunity or tolerance: opposing functional programs induced in human monocytes after engagement of various pattern recognition receptors. *Clin. Vaccine Immunol.* 21, 534–545. <https://doi.org/10.1128/CVI.00688-13>.
7. Murphy, D.M., Cox, D.J., Connolly, S.A., Breen, E.P., Brugman, A.A.I., Phelan, J.J., Keane, J., and Basdeo, S.A. (2023). Trained immunity is induced in humans after immunization with an adenoviral vector COVID-19 vaccine. *J. Clin. Invest.* 133, e162581. <https://doi.org/10.1172/JCI162581>.
8. van der Heijden, C.D.C.C., Groh, L., Keating, S.T., Kaffa, C., Noz, M.P., Kersten, S., van Herwaarden, A.E., Hoischen, A., Joosten, L.A.B., Timmers, H.J.L.M., et al. (2020). Catecholamines induce trained immunity in monocytes in vitro and in vivo. *Circ. Res.* 127, 269–283. <https://doi.org/10.1161/CIRCRESAHA.119.315800>.
9. Domínguez-Andrés, J., Novakovic, B., Li, Y., Scicluna, B.P., Gresnigt, M. S., Arts, R.J.W., Oosting, M., Moorlag, S.J.C.F.M., Groh, L.A., Zwaag, J., et al. (2019). The Itaconate Pathway Is a Central Regulatory Node Linking Innate Immune Tolerance and Trained Immunity. *Cell Metab.* 29, 211–220.e5. <https://doi.org/10.1016/j.cmet.2018.09.003>.

- Koeken, V.A.C.M., de Bree, L.C.J., Mourits, V.P., Moorlag, S.J.C.F.M., Walk, J., Cirovic, B., Arts, R.J.W., Jaeger, M., Dijkstra, H., Lemmers, H., et al. (2020). BCG vaccination in humans inhibits systemic inflammation in a sex-dependent manner. *J. Clin. Invest.* **130**, 5591–5602. <https://doi.org/10.1172/JCI133935>.
- Homeck Johnston, C.J.H., Ledwith, A.E., Lundahl, M.L.E., Charles-Messance, H., Hackett, E.E., O'Shaughnessy, S.D., Clegg, J., Prendeville, H., McGrath, J.P., Walsh, A.M., et al. (2024). Recognition of yeast β -glucan particles triggers immunometabolic signaling required for trained immunity. *iScience* **27**, 109030.
- Biggar, S.R., and Crabtree, G.R. (2001). Cell signaling can direct either binary or graded transcriptional responses. *EMBO J.* **20**, 3167–3176. <https://doi.org/10.1093/emboj/20.12.3167>.
- Ko, M.S., Nakauchi, H., and Takahashi, N. (1990). The dose dependence of glucocorticoid-inducible gene expression results from changes in the number of transcriptionally active templates. *EMBO J.* **9**, 2835–2842. <https://doi.org/10.1002/j.1460-2075.1990.tb07472.x>.
- Becskei, A., S eraphin, B., and Serrano, L. (2001). Positive feedback in eukaryotic gene networks: cell differentiation by graded to binary response conversion. *EMBO J.* **20**, 2528–2535. <https://doi.org/10.1093/emboj/20.10.2528>.
- Podtschaske, M., Benary, U., Zwinger, S., H ofer, T., Radbruch, A., and Baumgrass, R. (2007). Digital NFATc2 activation per cell transforms graded T cell receptor activation into an all-or-none IL-2 expression. *PLoS One* **2**, e935. <https://doi.org/10.1371/journal.pone.0000935>.
- K ock, J., Kreher, S., Lehmann, K., Riedel, R., Bardua, M., Lischke, T., Jargosch, M., Haftmann, C., Bendfeldt, H., Hatam, F., et al. (2014). Nuclear factor of activated T cells regulates the expression of interleukin-4 in Th2 cells in an all-or-none fashion. *J. Biol. Chem.* **289**, 26752–26761. <https://doi.org/10.1074/jbc.M114.587865>.
- Fuhrmann, F., Lischke, T., Gross, F., Scheel, T., Bauer, L., Kalim, K.W., Radbruch, A., Herzelt, H., Hutfloff, A., and Baumgrass, R. (2016). Adequate immune response ensured by binary IL-2 and graded CD25 expression in a murine transfer model. *eLife* **5**, e20616. <https://doi.org/10.7554/eLife.20616>.
- Liu, T., Yamaguchi, Y., Shirasaki, Y., Shikada, K., Yamagishi, M., Hoshino, K., Kaisho, T., Takemoto, K., Suzuki, T., Kuranaga, E., et al. (2014). Single-cell imaging of caspase-1 dynamics reveals an all-or-none inflammasome signaling response. *Cell Rep.* **8**, 974–982. <https://doi.org/10.1016/j.celrep.2014.07.012>.
- Shalek, A.K., Satija, R., Shuga, J., Trombetta, J.J., Gennert, D., Lu, D., Chen, P., Gertner, R.S., Gaublomme, J.T., Yosef, N., et al. (2014). Single-cell RNA-seq reveals dynamic paracrine control of cellular variation. *Nature* **510**, 363–369. <https://doi.org/10.1038/nature13437>.
- Sheu, K.M., Pimplaskar, A., and Hoffmann, A. (2024). Single-cell stimulus-response gene expression trajectories reveal the stimulus specificities of dynamic responses by single macrophages. *Mol. Cell* **84**, 4095–4110.e6. <https://doi.org/10.1016/j.molcel.2024.09.023>.
- Mu oz-Rojas, A.R., Kelsey, I., Pappalardo, J.L., Chen, M., and Miller-Jensen, K. (2021). Co-stimulation with opposing macrophage polarization cues leads to orthogonal secretion programs in individual cells. *Nat. Commun.* **12**, 301. <https://doi.org/10.1038/s41467-020-20540-2>.
- Tiemeijer, B.M., Heester, S., Sturtewagen, A.Y.W., Smits, A.I.P.M., and Tel, J. (2023). Single-cell analysis reveals TLR-induced macrophage heterogeneity and quorum sensing dictate population wide anti-inflammatory feedback in response to LPS. *Front. Immunol.* **14**, 1135223. <https://doi.org/10.3389/fimmu.2023.1135223>.
- Kellogg, R.A., Tian, C., Lipniacki, T., Quake, S.R., and Tay, S. (2015). Digital signaling decouples activation probability and population heterogeneity. *eLife* **4**, e08931. <https://doi.org/10.7554/eLife.08931>.
- Jain, N., Goyal, Y., Dunagin, M.C., Cote, C.J., Mellis, I.A., Emert, B., Jiang, C.L., Dardani, I.P., Reffsin, S., Arnett, M., et al. (2024). Retrospective identification of cell-intrinsic factors that mark pluripotency potential in rare somatic cells. *Cell Syst.* **15**, 109–133.e10. <https://doi.org/10.1016/j.cels.2024.01.001>.
- Reffsin, S., Miller, J., Ayyanathan, K., Dunagin, M.C., Heyman, Y., Jain, N., Schultz, D.C., Cherry, S., and Raj, A. (2026). Single-cell susceptibility to viral infection is driven by variable cell states. *Cell* **189**, 179–195.e21. <https://doi.org/10.1016/j.cell.2025.10.021>.
- Symmons, O., and Raj, A. (2016). What's Luck Got to Do with It: Single Cells, Multiple Fates, and Biological Nondeterminism. *Mol. Cell* **62**, 788–802. <https://doi.org/10.1016/j.molcel.2016.05.023>.
- Zhang, B., Moorlag, S.J.C.F.M., Dom nguez-Andr s, J., Bulut,  ., Kilic, G., Liu, Z., van Crevel, R., Xu, C.-J., Joosten, L.A.B., Netea, M.G., et al. (2022). Single-cell RNA sequencing reveals induction of distinct trained-immunity programs in human monocytes. *J. Clin. Invest.* **132**, e147719. <https://doi.org/10.1172/JCI147719>.
- Kong, L., Moorlag, S.J.C.F.M., Lefkovith, A., Li, B., Matzaraki, V., van Ernt, L., Kang, H.A., Latorre, I., Jaeger, M., Joosten, L.A.B., et al. (2021). Single-cell transcriptomic profiles reveal changes associated with BCG-induced trained immunity and protective effects in circulating monocytes. *Cell Rep.* **37**, 110028. <https://doi.org/10.1016/j.celrep.2021.110028>.
- Cheong, J.-G., Ravishankar, A., Sharma, S., Parkhurst, C.N., Grassmann, S.A., Wingert, C.K., Laurent, P., Ma, S., Paddock, L., Miranda, I.C., et al. (2023). Epigenetic memory of coronavirus infection in innate immune cells and their progenitors. *Cell* **186**, 3882–3902.e24. <https://doi.org/10.1016/j.cell.2023.07.019>.
- Moorlag, S.J.C.F.M., Folkman, L., ter Horst, R., Krausgruber, T., Barreca, D., Schuster, L.C., Fife, V., Matzaraki, V., Li, W., Reichl, S., et al. (2024). Multi-omics analysis of innate and adaptive responses to BCG vaccination reveals epigenetic cell states that predict trained immunity. *Immunity* **57**, 171–187.e14. <https://doi.org/10.1016/j.immuni.2023.12.005>.
- Messina, N.L., Netea, M.G., and Curtis, N. (2020). The impact of human single nucleotide polymorphisms on *Bacillus Calmette-Gu rin* responses. *Vaccine* **38**, 6224–6235. <https://doi.org/10.1016/j.vaccine.2020.07.032>.
- Knight, H.R., Ketter, E., Ung, T., Weiss, A., Ajit, J., Chen, Q., Shen, J., Ip, K. M., Chiang, C.-Y., Barreiro, L., et al. (2024). High-throughput screen identifies non-inflammatory small molecule inducers of trained immunity. *Proc. Natl. Acad. Sci. USA* **121**, e2400413121. <https://doi.org/10.1073/pnas.2400413121>.
- Bekkering, S., Blok, B.A., Joosten, L.A.B., Riksen, N.P., van Crevel, R., and Netea, M.G. (2016). In Vitro Experimental Model of Trained Innate Immunity in Human Primary Monocytes. *Clin. Vaccine Immunol.* **23**, 926–933. <https://doi.org/10.1128/CI.00349-16>.
- Sun, S., Aguirre-Gamboa, R., and Barreiro, L.B. (2023). Transmission of stimulus-induced epigenetic changes through cell division is coupled to continuous transcription factor activity. *Front. Immunol.* **14**, 1129577. <https://doi.org/10.3389/fimmu.2023.1129577>.
- O'Farrell, A., Niu, Z., Li, J., Van Eyndhoven, L.C., Sarma, K., and Raj, A. (2026). Human Macrophages Encode Stimulus-Specific Information of Prior Exposures Through Trained Immunity. *Cell Syst.* **17**, 101647. <https://doi.org/10.1016/j.cels.2026.101647>.
- Moorlag, S.J.C.F.M., R oring, R.J., Joosten, L.A.B., and Netea, M.G. (2018). The role of the interleukin-1 family in trained immunity. *Immunol. Rev.* **287**, 28–39. <https://doi.org/10.1111/imr.12617>.
- Sharif, O., Bolshakov, V.N., Raines, S., Newham, P., and Perkins, N.D. (2007). Transcriptional profiling of the LPS induced NF-kappaB response in macrophages. *BMC Immunol.* **8**, 1.
- Bagnall, J., Rowe, W., Alachkar, N., Roberts, J., England, H., Clark, C., Platt, M., Jackson, D.A., Muldoon, M., and Paszek, P. (2020). Gene-Specific Linear Trends Constrain Transcriptional Variability of the Toll-like Receptor Signaling. *Cell Syst.* **11**, 300–314.e8. <https://doi.org/10.1016/j.cels.2020.08.007>.
- Divangahi, M., Aaby, P., Khader, S.A., Barreiro, L.B., Bekkering, S., Chavakis, T., van Crevel, R., Curtis, N., DiNardo, A.R., Dominguez-Andres, J., et al. (2021). Trained immunity, tolerance, priming and differentiation: distinct immunological processes. *Nat. Immunol.* **22**, 2–6. <https://doi.org/10.1038/s41590-020-00845-6>.

40. Padovan-Merhar, O., Nair, G.P., Biaisch, A.G., Mayer, A., Scarfone, S., Foley, S.W., Wu, A.R., Churchman, L.S., Singh, A., and Raj, A. (2015). Single mammalian cells compensate for differences in cellular volume and DNA copy number through independent global transcriptional mechanisms. *Mol. Cell* 58, 339–352. <https://doi.org/10.1016/j.molcel.2015.03.005>.
41. Raj, A., and van Oudenaarden, A. (2008). Nature, nurture, or chance: stochastic gene expression and its consequences. *Cell* 135, 216–226. <https://doi.org/10.1016/j.cell.2008.09.050>.
42. Ferreira, A.V., Domínguez-Andrés, J., and Netea, M.G. (2022). The Role of Cell Metabolism in Innate Immune Memory. *J. Innate Immun.* 14, 42–50. <https://doi.org/10.1159/000512280>.
43. Fanucchi, S., Domínguez-Andrés, J., Joosten, L.A.B., Netea, M.G., and Mhlanga, M.M. (2021). The Intersection of Epigenetics and Metabolism in Trained Immunity. *Immunity* 54, 32–43. <https://doi.org/10.1016/j.immuni.2020.10.011>.
44. Arts, R.J.W., Carvalho, A., La Rocca, C., Palma, C., Rodrigues, F., Silvestre, R., Kleinnijenhuis, J., Lachmandas, E., Gonçalves, L.G., Belinha, A., et al. (2016). Immunometabolic Pathways in BCG-Induced Trained Immunity. *Cell Rep.* 17, 2562–2571. <https://doi.org/10.1016/j.celrep.2016.11.011>.
45. Cheng, S.-C., Quintin, J., Cramer, R.A., Shepardson, K.M., Saeed, S., Kumar, V., Giamarellos-Bourboulis, E.J., Martens, J.H.A., Rao, N.A., Aghajanirofeh, A., et al. (2014). mTOR- and HIF-1 α -mediated aerobic glycolysis as metabolic basis for trained immunity. *Science* 345, 1250684. <https://doi.org/10.1126/science.1250684>.
46. Emert, B.L., Cote, C.J., Torre, E.A., Dardani, I.P., Jiang, C.L., Jain, N., Shaffer, S.M., and Raj, A. (2021). Variability within rare cell states enables multiple paths toward drug resistance. *Nat. Biotechnol.* 39, 865–876. <https://doi.org/10.1038/s41587-021-00837-3>.
47. Niu, Z., Bruyère, T., Manthey, D., Li, J., O'Farrell, A., and Raj, A. (2025). NimbusImage: a cloud-computing platform for image analysis. *Nat. Methods* 23, 6–8. <https://doi.org/10.1038/s41592-025-02942-6>.
48. Niu, Z., O'Farrell, A., Li, J., Reffsin, S., Jain, N., Dardani, I., Goyal, Y., and Raj, A. (2025). Piscis: A loss estimator of the F1 score enables accurate spot detection in fluorescence microscopy images via deep learning. *Cell Syst.* 16, 101448. <https://doi.org/10.1016/j.cels.2025.101448>.
49. Raj, A., van den Bogaard, P., Rifkin, S.A., van Oudenaarden, A., and Tyagi, S. (2008). Imaging individual mRNA molecules using multiple singly labeled probes. *Nat. Methods* 5, 877–879. <https://doi.org/10.1038/nmeth.1253>.

STAR★METHODS

KEY RESOURCES TABLE

REAGENT or RESOURCE	SOURCE	IDENTIFIER
Biological samples		
Human monocytes from apheresis product of healthy donors	University of Pennsylvania Human Immunology Core	See Table S1
Chemicals, peptides, and recombinant proteins		
β -D-Glucan	Thomas Scientific	C940X31
Muramyl Dipeptide (MDP)	Invivogen	tlrl-mdp
Lipopolysaccharide (LPS)	Invitrogen	501122025
Deposited data		
Published scRNAseq dataset of human monocytes following in vivo BCG vaccination	Kong et al. ²⁸	GEO: GSE184241
Oligonucleotides		
Oligonucleotides for single-molecule RNA FISH	IDT	See Table S2
Software and algorithms		
RNA FISH Probe Design	Laboratory of Arjun Raj	https://github.com/arjunrajlaboratory/ProbeDesign
NimbusImage	Laboratory of Arjun Raj; Niu et al. ⁴⁷	https://github.com/arjunrajlaboratory/NimbusImage
Piscis	Laboratory of Arjun Raj; Niu et al. ⁴⁸	https://github.com/zjniu/Piscis
Code for analysis and figure generation	This paper	https://doi.org/10.5061/dryad.stjq2cjc

EXPERIMENTAL MODEL AND STUDY PARTICIPANT DETAILS

De-identified human immune cells were collected from the apheresis product of healthy donors at the Perelman School of Medicine at the University of Pennsylvania by the Human Immunology Core. Monocytes were isolated by negative selection with StemCell RosetteSep kits. Isolated monocytes were cultured in RPMI supplemented with 25mM HEPES, 1% penicillin/streptomycin, and 10% fetal bovine serum, and initially seeded at a density of 800,000 cells per milliliter in Cellvis 24 well glass imaging plates (Fisher NC0397150).

METHOD DETAILS

Induction of trained immunity

We followed an *in vitro* procedure of training commonly used in literature.³³ We introduced training ligands at the following concentrations: β -Glucan at 5 μ g/mL, and MDP at 1 μ g/mL. We chose these doses based on thorough comparison to published literature. To generate trained cells, we stimulated with training ligand during the first 24 hours of culture, while untrained cells received no stimulation. After 24 hours, we removed the training ligand by washing all wells (including untrained controls) twice with PBS, then allowed the cells to rest for five additional days, during which time the cells differentiated into monocyte-derived macrophages. On the sixth day of culture, we evaluated trained cells before or after secondary stimulation. Stimulation on day six with lipopolysaccharide (LPS) was at a dose of 100 ng/mL.

Single-molecule RNA fluorescence in-situ hybridization (RNA FISH) image acquisition

Oligonucleotides complementary to the transcripts for *TNF*, *IL1 β* , *CXCL10*, and *IL6* were designed using custom Matlab software (<https://github.com/arjunrajlaboratory/ProbeDesign>) and purchased from IDT. Due to the short length of these transcripts, we included the 3' UTR in each target sequence, to generate a total of 24 oligonucleotide probes per gene. Full sequences for each of these probes can be found in [Table S2](#). To generate fluorescent probes, we first added an amine group to the 3' end of each oligonucleotide using terminal transferase (TDT), then coupled to either CY3, Alexa 594, or Atto 700 dye.

Single-molecule RNA FISH was performed as described previously.⁴⁹ Briefly, cells were fixed in 4% paraformaldehyde for 10 minutes, then permeabilized using 70% ethanol overnight at 4°C. Immediately before probe addition, cells were briefly washed in 5% sodium dodecyl sulfate (SDS) for 1 minute to reduce autofluorescence.

To perform *in situ* hybridization, we diluted probes in hybridization buffer (10% formamide and 10% dextran sulfate in 2X saline sodium citrate (SSC) buffer) before incubating overnight at 37°C covered with a glass coverslip. Cells were then stained with DAPI for 30 minutes, then imaged in 2X saline sodium citrate (SSC) buffer. Samples were imaged across 5 Z-planes on an inverted Nikon TI-E microscope at 60X magnification.

Single-molecule RNA fluorescence in-situ hybridization (RNA FISH) image analysis

RNA FISH images were analyzed in the custom imaging software NimbusImage.⁴⁷ NimbusImage is an open-source, in-browser program that allows for direct visualization and analysis of large imaging datasets, and includes in-built analysis tools such as Cellpose, Segment-Anything, and Piscis.

Images were uploaded to NimbusImage, and cell cytoplasm was manually segmented using the “Manual Blob Annotation” tool. Morphology measurements for these annotations were calculated using the “Blob Metrics” tool.

RNA FISH spots (one spot is equivalent to one mRNA transcript) were identified across all Z planes using the deep learning algorithm Piscis.⁴⁸ Piscis is a deep neural network classification algorithm that employs a novel loss function (the SmoothF1 loss) to account for class imbalance inherent to RNA FISH spot detection during training, ensuring accurate spot detection. Following identification, spots were counted and assigned to each cell using the “Point Count 3D Projection” tool in NimbusImage. Proportions of cells expressing each gene were calculated using a threshold of 1 spot per cell after manual noise correction. When calculating spot count for expressing cells for *TNF*, *IL1β*, *IL6* and *CXCL10*, we first filtered to only include cells with at least one transcript, then normalized by cell area, plotting as spots per square micron.

For local density calculations in Figure S4B, we relied on the natural variations in cell density present across the plate of cells. Primary monocytes began their culture in suspension, and settled onto the bottom of the plate as they differentiated, leaving the center of the well slightly more dense than the periphery by day six of culture. We also observed minor differences in macrophage density across cells from different donors. As such, to determine local cell density, we counted the number of cells present within a single microscopy image frame.

Single cell RNA sequencing data analysis

We downloaded a publicly available scRNAseq dataset originally published in Kong et al.,²⁸ of human monocytes from three individuals before, two weeks after, and three months after BCG vaccination. We downloaded the data as raw sequencing counts, then used the same preprocessing steps used in²⁸ (filtered out cells with less than 200 unique gene counts and genes detected in less than three cells). We then used a centered log-ratio transform before differential expression analysis using *Seurat* (also as described in Kong et al.²⁸).

Of the 1,710 cells in the full dataset, we filtered to remove the cells sampled at resting state (before any restimulation), leaving the 855 cells sequenced four hours after *ex vivo* restimulation with LPS. We then plotted the normalized expression of each gene of interest, and calculated the p-value of differential expression between trained vs untrained cells using the *t.test()* function.

QUANTIFICATION AND STATISTICAL ANALYSIS

To calculate statistical significance across proportions of *IL6* and *CXCL10* first responders in trained and untrained cells, we used the following equation: $z = \frac{(p_{trained} - p_{untrained})}{\sqrt{p_{total}(1 - p_{total}) \left(\frac{1}{n_{trained}} + \frac{1}{n_{untrained}} \right)}}$, where $p_{trained}$ is the proportion of first responder cells in the trained popu-

lation, $p_{untrained}$ is the proportion of first responders in the untrained population, p_{total} is the overall sample proportion, and $n_{trained}$ and $n_{untrained}$ are the sample sizes. We then used the *pnorm()* function in R to convert the z-score to a p-value, using a two-tailed test for statistical significance.

To calculate statistical significance for *TNF*, *IL1β*, *IL6*, and *CXCL10* expression per cell, we calculated the number of spots per square micron in each expressing cell, before using the *t.test()* function in R to calculate the p-value for a two-tailed test for statistical significance.

For the log₂ odds ratio calculation between *IL6* and *CXCL10* expression (at two hours post restimulation in Figure 2E, Figure S3, and at six hours post restimulation in Figure S3B) we used the following equation: $OR = \frac{\text{Number of Cells Expressing Neither Gene} * \text{Number of Cells Expressing Both Genes}}{\text{Number of Cells Expressing IL6 Only} * \text{Number of Cells Expressing CXCL10 Only}}$.

For one of the 39 conditions assessed at two hours (Donor ND608B, untrained condition), we artificially added one count to the *IL6* only group, to prevent a divide-by-zero error. For one of the 9 conditions assessed at six hours (Donor ND624, β-Glucan-trained condition), we artificially added one count to the *IL6* only group and one count to the neither gene group, to prevent a divide-by-zero error and to allow the log₂ to be calculated.

Spearman correlation coefficients were calculated using the *cor()* function in R, with the method set to ‘spearman’. We then bootstrapped the result using *boot()* 1000 times, to calculate the bootstrapped standard error of the correlation.